ELSEVIER

Journal of Organometallic Chemistry 650 (2002) 114–122

Journal of Organometallic Chemistry

www.elsevier.com/locate/jorganchem

Synthesis and characterization of planarly chiral nonbridged bis(1-*R*-indenyl) zirconium dichloride complexes and X-ray structure of *rac*-[(η^5-C_9H_6-1-$C(CH_3)_2$–*o*-C_6H_4–OCH_3)$_2ZrCl_2$]·THF

Haiyan Ma, Jiling Huang, Yanlong Qian *

Laboratory of Organometallic Chemistry, East China University of Science and Technology, P.O. Box. 310, 130 Meilong Road, Shanghai 200237, China

Received 15 November 2001; received in revised form 15 January 2002; accepted 16 January 2002

Abstract

Reactions of the lithium salts of 3-substituted indenes **1**, **2** with $ZrCl_4(THF)_2$ gave two series of nonbridged bis(1-substituted)indenyl zirconocene dichloride complexes. Fractional recrystallization from THF–petroleum ether furnished the pure racemic and mesomeric isomers of [(η^5-C_9H_6-1-$C(R^1)(R^2)$–*o*-C_6H_4–OCH_3)$_2ZrCl_2$]·*n*THF ($R^1 = R^2 = CH_3$, $n = 1$, *rac*-**1a** and *meso*-**1b**; $R^1 = CH_3$, $R^2 = C_2H_5$; $n = 0.5$ or 0, *rac*-**2a** and *meso*-**2b**), respectively. Complex **1a** was further characterized by X-ray diffraction to have a C_2 symmetrically racemic structure, where the six-member rings of the indenyl parts are oriented laterally and two *o*-CH_3O–C_6H_4–$C(CH_3)_2$– substituents are oriented to the open side of the metallocene (Ind: bis-lateral, *anti*; Substituent: bis-central, *syn*). The four zirconocene complexes are highly symmetrical in solution as characterized by room temperature ^{1}H-NMR, however ^{1}H–^{1}H NOESY of *meso*-**1b** shows that some of the NOE interactions arise from the two separated indenyl parts of the same molecule, which can only be explained well by taking into account the torsion isomers in solution. © 2002 Published by Elsevier Science B.V.

Keywords: Zirconocene; Planar chirality; Nonbridged bis(1-*R*-indenyl) ligand; Crystal structure

1. Introduction

The discovery of the extremely active Group 4 bent metallocene/aluminoxane catalysts has led to remarkable research activities in homogenous catalytic α-olefin polymerization [1–5]. The majority of this work has been carried out with the *ansa*-metallocene derived catalyst systems, since such bridged metallocene catalysts produced highly isotactic or syndiotactic polypropylene with very high activities [6–9]. It is further proved that the stereoselectivity during the process of polymerization is raised from the specific model of the attachment of the Group 4 metal atom to the enantiotropic *R* or *S* faces of the planarly prochiral 1-substituted indenyl ligand moieties; the intrinsic chirality properties have no direct relation with the bridge-part. Waymouth's nonbridged and oscillating bis(2-substituted) indenyl zirconocene complexes acted as good examples of this point: bulky substituents enabled these metallocenes to polymerize sections of atactic and isotactic polypropylene in the same polymer chain, which was thought to have been caused by the interconversion of the molecular structure between mesomeric and racemic conformers [10].

From features associated with the metal–indenyl torsion potential, nonbridged bis(1-substituted)indenyl zirconocenes do not reveal fundamentally stereochemical differences to *ansa*-metallocenes [11]; prochiral 1-substituted indenyl ligands can also yield two diastereoisomers. *R*,*R* and *S*,*S* attachments give rise to the two racemic enantiomers, whereas a *R*,*S* attachment gives the *meso*-diastereoisomer [12]. It could be conceived that nonbridged bis(1-substituted)indenyl zirconocene complexes might also have some interesting properties towards the polymerization of α-olefins. However, research on the synthesis and application of such complexes in polymerization is limited; only a few publications by Erker and a few other groups appeared in the open literature when compared to *ansa*-metallocenes [11–16].

* Corresponding author. Tel./fax: +86-21-6470-2573.
E-mail address: qianling@online.sh.cn (Y. Qian).

0022-328X/02/$ - see front matter © 2002 Published by Elsevier Science B.V.
PII: S0022-328X(02)01197-X

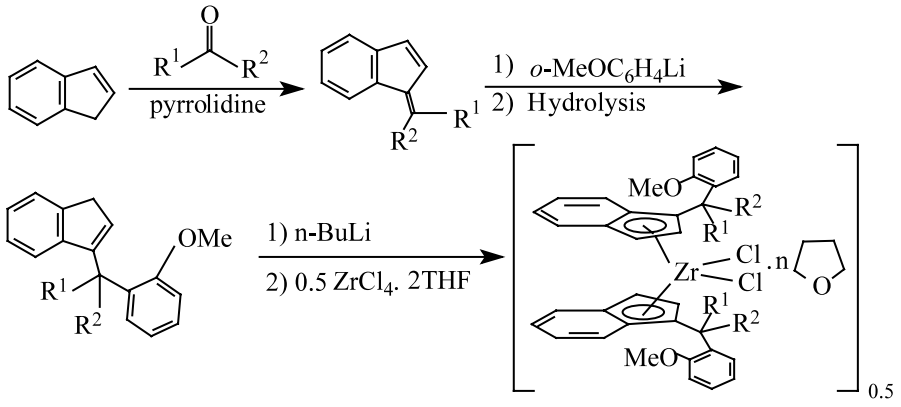

1 $R^1 = R^2 = Me$

2 $R^1 = Me$, $R^2 = Et$

rac-**1a** and *meso*-**1b**(n=1)

rac-**2a** and *meso*-**2b**(n=0.5 or 0)

Scheme 1.

In this work we synthesized two bulky-group-substituted indenes 3-[*o*-CH_3O–C_6H_4–$C(R^1)(R^2)$]–C_9H_6 ($R^1 = R^2 = CH_3$, **1**; $R^1 = CH_3$, $R^2 = C_2H_5$, **2**), and used them in the complexation with $ZrCl_4(THF)_2$. Two series of racemic/mesomeric, nonbridged bis(1-substituted)-indenyl zirconium dichloride complexes were obtained and separated successfully through fractional recrystallization. The investigation of their behaviors towards the polymerization of α-olefin is still in progress.

2. Results and discussion

2.1. Synthesis of zirconocene complexes

Nucleophilic attacks of the lithium reagents at the positively polarized exo carbon of the corresponding benzofulvenes prepared according to the literature methods [17] and sequential hydrolysis gave the 3-substituted indenes, 3-[*o*-CH_3O–C_6H_4–$C(R^1)(R^2)$]–C_9H_6 ($R^1 = R^2 = CH_3$, **1**; $R^1 = CH_3$, $R^2 = C_2H_5$, **2**) in high yields, respectively. Then the substituted indenes **1**, **2** were treated with *n*-butyllithium and 0.5 equivalent of $ZrCl_4(THF)_2$ in sequence to afford mixture of *rac*- and *meso*-diastereoisomers **1a**/**1b** (*rac*:*meso*, about 55:45) or **2a**/**2b** (*rac*:*meso*, about 60:40) in quite high yields (Scheme 1). Fractional crystallization of the mixtures from THF and petroleum ether fulfilled the separation of pure *rac*- and *meso*-isomers. However the net yields were quite low. The many fractional crystallization steps undertaken for the purification of these zirconocenes with quite similar properties incurred a heavy product-loss.

The solubility of the four zirconocene complexes in THF was initially good, but upon precipitation of the products from the solution, most of the cases as powder, it became difficult to dissolve them again, and a large amount of THF had to be used. It seemed that some aggregated structures might be formed during the process of the rapid precipitation. By using less concentrated solution, all of them could be separated as crystals, thus **1a** and **1b** were separated as THF-containing complexes, and **2a** was characterized as containing $\frac{1}{2}$ solvate THF per molecule, however **2b** was isolated without THF.

It is noticeable that there is a chiral sp^3 carbon in ligand **2**; after metallization by $ZrCl_4$, the 1-substituted indenyl leads to the planar chirality, thus in total there are four stereogenic elements in the same molecule. The formation of ten potential diastereoisomers (four pairs of racemic enantiomers, and two mesomeric isomers) is conceived. However, from the reaction, only three isomers (*rac*-**2a** and *meso*-**2b**) were isolated. No other isomer could be detected. Our previous results [18] showed the coordination of zirconium to this ligand was stereoselective, and the chirality in the α-carbon of the side chain controlled the planar chirality of the resulting complex[1]. According to this fact, we propose the isomers formed in the reaction are those with the ethyl group of the side chain locating against the six-member ring of the indenyl ligand.

2.2. Characterization of zirconocene complexes

The *rac*- and *meso*-diastereoisomers **1a**/**1b** or **2a**/**2b** are highly symmetrical in solution as characterized by ^{1}H-NMR. Although torsion isomers were reported for nonbridged bis(indenyl)zirconium complexes [11–14], the ligand rotation is generally too fast to be detected

[1] Zirconium complex [η^5:η^1-C_9H_6-1-$C(CH_3)(C_2H_5)$-*o*-C_6H_4–OCH_3]$ZrCl_3$·THF was obtained as single pair of enantiomers ((p*R*, *S*) and (p*S*, *R*)). Its crystal structure shows the ethyl group of the side chain is located against the six-member ring of the indenyl ligand.

Table 1
Selected ^{1}H-NMR spectra data for the bis(1-*R*-indenyl)zirconium dichloride complexes

Metallocene	Isomer	H-2	H-3	$\Delta\delta$ (H-2–H-3)
1a [a]	*rac*-	6.15	6.54	−0.39
1b	*meso*-	6.78	6.00	0.78
1c	*rac*-	6.32	6.48	−0.16
2a	*rac*-	6.14	6.63	−0.49
2b	*meso*-	6.88	6.07	0.81
Bis(1-^{i}Pr-Ind)$ZrCl_2$ [b]	*rac*-	5.91	5.90	0.01
	meso-	6.33	5.37	0.96
Bis(1-^{t}Bu-Ind)$ZrCl_2$ [b]	*rac*-	5.89	6.48	−0.59
	meso-	6.43	6.05	0.38
Bis(1-Bz-Ind)$ZrCl_2$ [b]	*rac*-	6.05	5.83	0.22
	meso-	6.29	5.29	1.00

[a] Assignment of stereochemistry made by X-ray crystallography.
[b] The data were cited from Ref. [13].

by room temperature scale ^{1}H-NMR, the *rac*-isomers are C_2 symmetrical and the *meso*-isomer has C_S symmetry in solution. The *rac*- and *meso*-diastereoisomeric complexes of **1a**/**1b** or **2a**/**2b** give rise to two different sets of ^{1}H-NMR resonances of the same general spectroscopic type and appearance, respectively. However, the *rac*- or *meso*-isomers can be readily distinguished from each other by the differing position of their H-2 and H-3 spectroscopy signals. For all of the metallocenes, the H-3 signal was identified as a doublet of doublets through its coupling to protons H-2 and H-7 (characterized by ^{1}H–^{1}H TOCSY); H-2 shows simple doublet through the coupling with H-3.

Comparing with the reported *rac*- and *meso*-bis(1-substituted)indenyl zirconocene complexes in Table 1, we find the signals of H-2 and H-3 in **1a** and **2a** have the same tendency as those in *rac*-bis(1-^{t}Bu-Ind)$ZrCl_2$ (this complex also contains a bulky substituent of *t*-butyl); the H-2 signals of them are all upfield from H-3. Furthermore, the H-2, H-3 signals in **1b**, **2b** and *meso*-bis(1-^{t}Bu–Ind)$ZrCl_2$ have the same tendency. Besides these two points, the result of Grimmer and his coworkers shows, the "inner pair" of H-2 and H-3 signals usually belongs to the *rac*-isomers [13], thus we tentatively assigned complexes **1a**, **2a** as racemic isomers, and complexes **1b**, **2b** as mesomeric isomers. The absolute stereochemical assignment for *rac*-**1a** was made possible by X-ray crystallography (vide infra).

In order to get more information about the stereochemical structures, ^{1}H–^{1}H NOESY of *meso*-**1b** was determined at room temperature. Fig. 1 shows clearly the NOE interactions within the molecule of *meso*-**1b**, H-2 and H-3 come into contact with H-4; the methyl groups of side chain also come into contact with H-2, H-3 and H-7. Our unpublished result [19] shows, in the mixed Cp–Ind zirconocene complex [(η^5-C_9H_6-1-$C(CH_3)_2$–*o*-C_6H_4–OCH_3)Cp]$ZrCl_2$, only H-3 of the in-

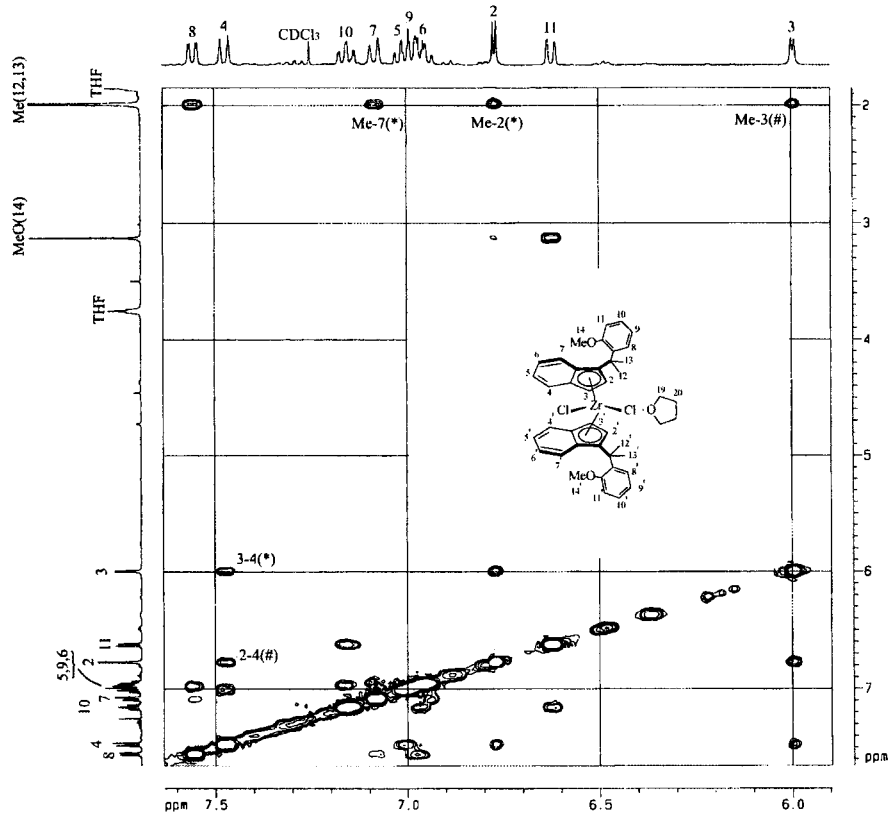

Fig. 1. ^{1}H–^{1}H NOESY of *meso*-**1b** ($CDCl_3$, 298 K, 400 MHz).

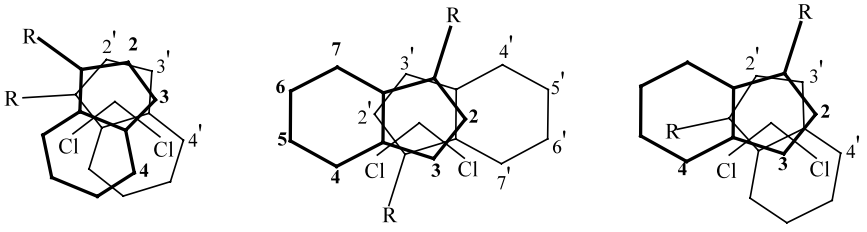

meso-**A** *meso*-**B** *meso*-**C**

Scheme 2.

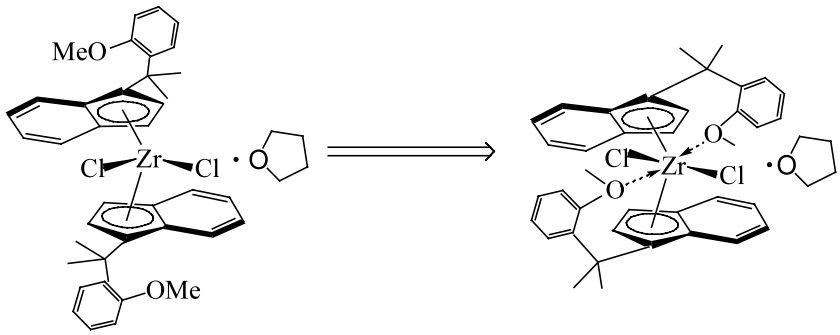

rac-**1a** *rac*-**1c**

Scheme 3.

denyl ligand comes into contact with H-4, no NOE interaction exists between H-2 and H-4; and the methyl groups of the side chain only come into contact with H-2 and H-7. No NOE interaction exists between methyl group and H-3 (adopting the same numbering method as this work), thus we infer that the interactions of H-2 and H-4, methyl groups and H-3 can only arise from the two separated indenyl ligands within the same molecule; they are interligand NOE contacts.

As for the rest of the NOE contacts, we of course could not simply assign them as intraligand interactions; to a certain extent, some of them may also arise from the two separated indenyl ligands. Some relevant results of NOE contacts concerning the interligand interactions of two sterically hindered Cp-based zirconocene complexes were reported recently by Grimmond and his co-workers [20].

Only taking into account the C_s symmetric structure of *meso*-**1b** in solution, it is difficult to explain the two mentioned interligand NOE interactions. Generally, in the C_s symmetric structure, H-2 is located far away from H-4′, and methyl groups are also far away from H-3′; no interaction could be imagined. This inconsistency makes us go back to the torsion isomers. It is reported that at least three torsion isomers may exist for the *meso*-diastereoisomer of bis(1-substituted)indenyl metallocene complexes; their idealized structures could be depicted in Scheme 2 [11,12]. *meso*-**1b** should have similar torsion isomers in solution. In the structure of *meso*-**A**, H-2 is found to be located far away from the H-4′ (and also H-2′ and H-4), and so are the methyl groups of side chain and H-3′; thus there is little possibility that the interligand NOE interactions arise from this structure. However, the other two structures provide the possibility of these contacts, (1) in the structure of *meso*-**B**, methyl groups of the side chain could be located near to H-3′; (2) in the structure of *meso*-**C**, H-2 could be located near H-4′, and the methyl groups of the side chain could be located near H-3′; (3) at the same time, most of these hydrogen atoms are located in the narrow side of the bent structure; it is imaginable that there will be NOE interactions. We suggest here, although the C_s symmetric structure of *meso*-**1b** is characterized by room temperature ^{1}H-NMR, the interligand NOE contacts existing possibly in the torsion isomers could be detected under the same condition.

When we attempted to characterize complex *rac*-**1a** through the same method, it proved to be unsuccessful. *rac*-**1a** was not stable enough to fulfil the determination of ^{1}H–^{1}H NOESY in solution. During the measurement, the H-signal of methoxyl groups had a significant downshift from δ3.15 to 3.89 gradually, and this transformation achieved completion after 1 day. It seemed that the methoxyl groups of the two substituents tended to coordinate to the zirconium center [21], and formed a new complex **1c**[2]. The same tendency of coordination

[2] The coordinated complex **1c** can be characterized by ^{1}H-NMR (δ, $CDCl_3$): 7.31 (m, 2H), 7.13 (m, 4H), 7.0 (m, 2H), 6.95 (m, 4H), 6.88 (t, 2H), 6.78 (m, 2H), 6.48 (dd, 2H), 6.32 (d, 2H), 3.89 (s, 6H), 1.49 (s, 6H), 1.08 (s, 6H). It is an average structure.

was also found in complex *rac*-**2a**[3]. Compared with other zirconocene complexes in Table 1, the H-2 and H-3 signals of **1c** have the same trend as those in *rac*-**1a**, *rac*-**2a** and *rac*-bis(1-^{t}Bu–Ind)$ZrCl_2$; thus we assigned its structure as racemic isomer (Scheme 3).

2.3. Crystal structure of *rac*-**1a**

Single crystals of *rac*-**1a** suitable for X-ray diffraction were obtained from THF–petroleum ether (Fig. 2). The crystal structure of *rac*-**1a** reveals the existence of two unique molecules in a 1:1 ratio as racemic enantiomers, which crystallize in the orthorhombic space group *Pbcn* (# 60) with a solvate THF molecule. Table 2 summarizes the bonding parameters of it. *rac*-**1a** has C_2 symmetry, with the zirconium atom in a pseudotetrahedral environment formed by the two chlorine ligands and two η^5-coordinated indenyl ligands. The corresponding bond lengths and angles of the two indenyl-parts in one molecule are identical. The Zr–C bond lengths of five member rings range between 2.427(5) and 2.696(4) Å ($\Delta = 0.269$ Å). This scope is wider than the nonbridged 1- or 2-substituted bis(indenyl) zirconocene complexes ($\Delta = 0.1$–0.16 Å) reported in the literature [11–14,22–24] and is closer to the *ansa*-bis(indenyl) zirconocene complexes ($\Delta = 0.18$–0.25 Å) [9]. The Zr–C distance to the substituted carbon is longer than the other Zr–(CH) distances (Zr–C(9) > Zr–C(8) > Zr–C(7)); but the longest Zr–C distance is Zr–C(1) (2.696(4) Å), where C(1) is adjacent to C(9) and belongs to the six-member ring. It suggests that the bulky substituent of $–C(CH_3)_2–o\text{-}C_6H_4–OCH_3$ group leads to the unsymmetrical bonding of Zr atom to the carbons of the five-member ring significantly.

The Zr–Cl distances of 2.4183(14) are within the range observed previously for other bis(indenyl)-zirconium dichlorides (2.407(1)–2.465(2) Å) [11–14,22–25]. However, the Cl–Zr–Cl* angle of 101.43(8)° is notably larger than the common value for the nonbridged 1- or 2-substituted bis(indenyl) zirconium dichloride complexes (91–98.98 Å) and is close to the *ansa*-metallocenes [11–14,22–24] (Table 3). Resconi et al. reported that this value was a little sensitive to the steric hindrance of the ligands [9c]. In our case, the bigger value is most likely to be caused by the bulky substituents at C(9) and C(9*) of indenyl fragments. The bite angle of Cp(cnt)–Zr–Cp′(cnt) in *rac*-**1a** is 131.97°, which is in the range of normal nonbridged bis(1-subsituted)indenyl zirconocene complexes, and is much larger than the *ansa*-metallocene complexes. The two bulky substituents seem to have less influence on this factor, and also have less influence on the distance of Zr–Cp(cnt).

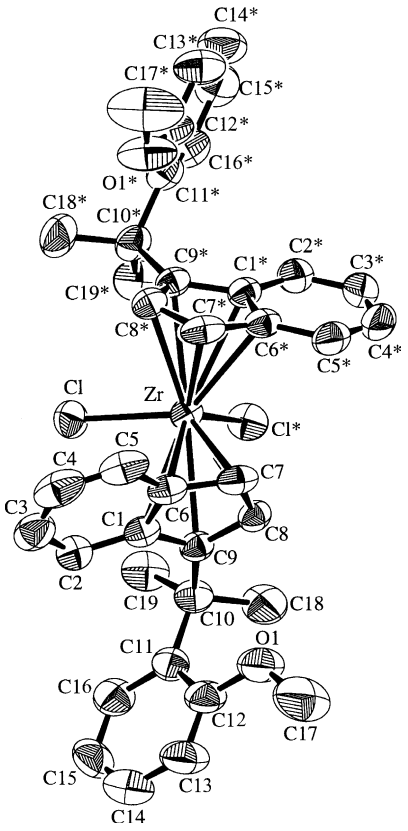

Fig. 2. Solid state structure of *rac*-**1a** (hydrogen atoms are omitted for clarity).

Table 2
Selected bond lengths (Å) and angles (°) for *rac*-**1a**

Bond lengths			
Zr–Cl	2.4183(14)	C(1)–C(6)	1.436(6)
Zr–Cl*	2.4183(14)	C(6)–C(7)	1.418(8)
Zr–C(1)	2.696(4)	C(7)–C(8)	1.390(7)
Zr–C(6)	2.546(4)	C(8)–C(9)	1.389(7)
Zr–C(7)	2.427(5)	C(9)–C(1)	1.432(7)
Zr–C(8)	2.519(5)	C(1)–C(2)	1.398(7)
Zr–C(9)	2.661(4)	C(2)–C(3)	1.370(8)
C(9)–C(10)	1.535(6)	C(3)–C(4)	1.430(10)
C(10)–C(11)	1.534(7)	C(4)–C(5)	1.322(9)
C(12)–O(1)	1.386(7)	C(5)–C(6)	1.395(7)
Zr–Cp(cnt)	2.274	O(1)–C(17)	1.425(7)
Bond angles			
Cl–Zr–Cl*	101.43(8)	C(1)–Zr–C(1*)	163.97(19)
C(7)–Zr–C(7*)	78.5(2)	Cl–Zr–C(7)	126.66(16)
C(9)–Zr–C(9*)	175.88(18)	Cl–Zr–C(9)	85.38(11)
Cp(cnt)–Zr–Cp′(cnt)	131.97		

Erker et al. [11,12] have proposed three possible solid-state conformers for nonbridged *rac*-bis(1-*R*-indenyl) zirconocene complexes (Scheme 4). From the top view of the crystal structure of *rac*-**1a** (Fig. 3) it is

[3] After being stored for a certain time (several months as solid state), the proton signal of the methoxyl groups in *rac*-**2a** also had a significant shift from δ 3.06 to 3.88. However the new complex cannot be characterized well by ^{1}H-NMR, since the transformation is not yet completed. Simple heating of the complex in solution cannot promote this procedure.

Table 3
Relevant bond lengths (Å) and angles (°) of different nonbridge and *ansa*-zirconocene complexes

Zirconocene	Lengths		Angles	
	Zr–Cl	Zr–Cp(cnt)	Cl–Zr–Cl	Cp(cnt)–Zr–Cp′(cnt)
rac-**1a**	2.4183(14)	2.274	101.43(8)	131.97
rac-[(1-Et-Ind)$_2$]ZrCl$_2$ [13] (*R*,*R*)	2.449(5)/2.434(4)	2.224	96.45(16)	132.72
rac-[(1-Ph-Ind)$_2$]ZrCl$_2$ [13]	2.429(7)	2.231	98.98(2)	128.66
[(1-Nem-Ind)$_2$]ZrCl$_2$ [11b] [a]	2.424(1)	–	91.6(1)	129.6
[(1-(*p*-F-Bz)-Ind)$_2$]ZrCl$_2$ [14]	2.417(3)/2.429(3)	2.218/2.242	94.6(1)	129.0
[(2-(3,5-Me$_2$-Ph-Ind)$_2$)ZrCl$_2$ [10a]	2.425(2)/2.430(2)	2.240/2.237	94.2(1)	130.1
[(2-(3,5-(CF$_3$)$_2$-Ph-Ind)$_2$)ZrCl$_2$ [10a]	2.415(1)/2.407(1)	2.400/2.233	94.5(1)	130.9
[(2-Men-Ind)$_2$]ZrCl$_2$ [22] [b]	2.4238(9)/2.4337(9)	2.314/2.234	93.98(3)	134.7
	2.4289(10)/2.4429(9)	2.232/2.240	91.91(3)	131.2
[(2-Morp-Ind)$_2$]ZrCl$_2$ [23] [a]	2.430(1)/2.462(1)	2.532	95.84(5)	132.5
rac-[CH$_2$(3-*t*-Bu-1-Ind)$_2$]ZrCl$_2$ [9c]	2.4122(12)	2.262	98.82(2)	117.62
rac-Me$_2$C(3-*t*-Bu-1-Ind)$_2$]ZrCl$_2$ [9a]	2.405(2)	–	98.69(9)	118.3
rac-Me$_2$C(3-Me$_3$Si-1-Ind)$_2$]ZrCl$_2$ [9a]	2.4205(4)	–	100.69(2)	117.4

[a] Nem = neomenthyl; Men = menthyl; Morp = morpholino.
[b] Two independent structures in the same crystal.

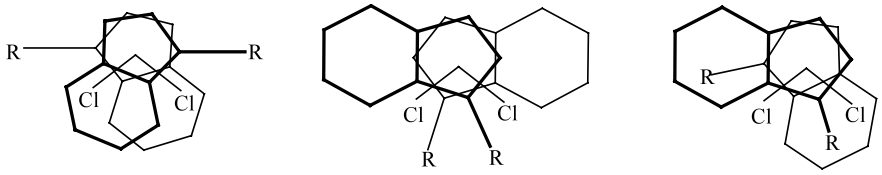

rac-**A** — Ind: bis-central, *syn*; R: bis-lateral, *anti*

rac-**B** — Ind: bis-lateral, *anti*; R: bis-central, *syn*

rac-**C** — Ind: central/lateral; R: central/lateral

Scheme 4.

found that the two –C(CH$_3$)$_2$–*o*-C$_6$H$_4$–OCH$_3$ substituents are *syn* orientated over the open side of the metallocene, and the two six-member rings of the indenyl parts are positioned laterally. This conformer is consistent with the idealized structure of *rac*-**B** [11–13]. Furthermore, the aromatic parts of the two substituents are orientated far away from the metallocene center (Fig. 1), which is thought to reasonably reduce the steric hindrance caused by *syn* orientation of the two substituents.

From the crystallographic data of *rac*-**1a**, we found that the strong steric hindrance caused by the two bulky substituents of –C(CH$_3$)$_2$–*o*-C$_6$H$_4$–OCH$_3$ and also by the two indenyl parts led to some structure features, which are more similar to those of *ansa*-bis(indenyl) zirconium dichloride complexes. So it is suggested that properly bulky substituents in the five-member rings of nonbridged metallocene might have similar influence on the metallocene structure as the bridge part does on the *ansa*-metallocene complex, which produces similar structure parameters.

The solvate THF molecule in *rac*-**1a** exists freely; no efficient interaction could be found between it and other parts of the molecule. From the ^{1}H-NMR spectroscopic data, the same conclusion could be made. The proton signals of THF in *rac*-**1a** are consistent with a free molecule, and so are those in the other two complexes, *meso*-**1b** and *rac*-**2a**.

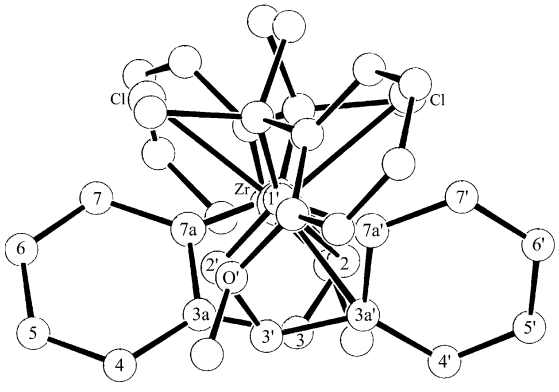

Fig. 3. The top view of *rac*-**1a** (hydrogen atoms are omitted for clarity, with different numbering system as Fig. 2).

3. Conclusions

Bulky-group-substituted indene ligands of 3-[*o*-CH_3O–C_6H_4–$C(R^1)(R^2)$]–C_9H_6 ($R^1 = R^2 = CH_3$, **1**; $R^1 = CH_3$, $R^2 = C_2H_5$, **2**) were synthesized and their lithiated salts reacted with $ZrCl_4(THF)_2$ to give correspondingly nonbridged bis(1-substituted)indenyl zirconium dichloride complexes. The *rac*- and *meso*-isomers **1a**/**1b** or **2a**/**2b** could be separated and purified by fractional recrystallization from THF and petroleum ether. Although the chiral sp^3 carbon in the side chain of ligand **2** was introduced, only one set of *rac*/*meso*-zirconocene complexes could be detected and separated. The chirality in the α-carbon of the side chain controlled the planar chirality of the resulting complex, which led to the reduction of isomers.

The absolute structure of **1a** was determined successfully by X-ray diffraction to be the racemic isomers; the two –$C(CH_3)_2$–*o*-C_6H_4–OCH_3 substituents in it are *syn* orientated over the open side of the bent structure, and the two six-member rings of the indenyl parts are positioned laterally. Furthermore, the aromatic parts of the two substituents are orientated far away from the metallocene center, which reasonably reduces the steric hindrance caused by *syn* orientation of the two substituents. **1b** is the mesomeric isomer. According to the spectroscopic characters of these zirconocene complexes, the racemic nature of **2a** and mesomeric nature of **2b** were assigned.

The four zirconocene complexes are highly symmetrical in solution as characterized by room temperature ^{1}H-NMR, but ^{1}H–^{1}H NOESY of *meso*-**1b** shows that some of the NOE interactions arise from the two separated indenyl parts of the same molecular, which can only be explained well by taking into account the torsion isomers in solution.

The racemic zirconocene complexes **1a** and **2a** are not stable enough structurally. The methoxyl groups of the side chain tended to coordinate to the metal center in solid state or in solution, which caused a significant shift of the proton signals of methoxyl groups from 3.15 to 3.89, or from 3.06 to 3.88, respectively. The coordinated product of *rac*-**1a** was well characterized by ^{1}H-NMR.

4. Experimental

All reactions were carried out under an inert atmosphere of dry Ar using standard Schlenk techniques. Reaction vessels were flame dried under vacuum then filled with Ar several times. Tetrahydrofuran, Et_2O, petroleum ether and *n*-hexane were distilled under Ar from purple or blue sodium/benzophenone ketyl according to the solvents prior to use. Dichloromethane was distilled from anhydrous P_2O_5 prior to use. Elemental analyses were performed with an EA-1106 microanalyzer. IR spectra were recorded in KBr using a Nicolet 5SXC or Nicolet Magna-IR 550 instrument. Mass spectra were carried out with a HP-5989A spectrometer at 70 eV. ^{1}H-NMR, ^{1}H–^{1}H TOCSY and NOESY were recorded on a Bruker 400MHz or Advance 500MHz instruments using $CDCl_3$ as solvent.

o-Bromoanisole [25], 6,6′-dimethyl-benzofulvene, and 6,6′-methyl,ethyl-benzofulvene [17] were prepared according to the literature procedures.

4.1. Synthesis of 3-[*o*-CH_3O–C_6H_4–$C(CH_3)_2$]–C_9H_6 (*1*)

To the solution of *o*-bromoanisole (0.143 mol, 26.7 g) in 100 ml *n*-hexane, was added dropwise the solution of *n*-BuLi (0.143 mol, 75 ml) in hexane. Plenty of white precipitates were produced. The obtained white precipitates of *o*-$CH_3OC_6H_4Li$ were filtrated and dissolved in Et_2O.

A solution of 6,6′-dimethyl-benzofulvene (0.123 mol, 19.2 g) in 50 ml Et_2O was then added dropwise at room temperature (r.t.) to the above lithium solution. The mixture was stirred overnight and then hydrolyzed. After work-up, **1** was obtained as pale orange crystals in 71% (23 g), m.p.: 89–91 °C. ^{1}H-NMR (δ, ppm, $CDCl_3$): 7.39 (m, 2H), 7.19 (ddd, 1H, $^3J = 8.1$ Hz, $^3J = 7.4$ Hz, $^4J = 1.68$ Hz), 7.03 (td, 1H, $^3J = 7.4$ Hz, $^3J = 7.4$ Hz, $^4J = 1.0$ Hz), 6.95 (m, 2H), 6.77 (dd, 1H, $^3J = 8.1$ Hz, $^4J = 1.1$ Hz), 6.70 (dd, 1H, $^3J = 7.7$ Hz, $^4J = 1.0$ Hz), 6.34 (t, 1H, $^3J = 2.2$ Hz), 3.46 (s, 3H), 3.35 (d, 2H, $^3J = 2.2$ Hz), 1.72 (s, 6H). MS (*m*/*z*): 264 (13, M^+), 149 (100, $M^+ - C_9H_7^\bullet$). IR (cm^{-1}, KBr): 3070m, 3000m, 2985m, 2970m, 1600m, 1580m, 1485s, 1460s, 1435s, 1396m, 1375m, 1355m, 1290m, 1245s, 1150m, 1085m, 1050m, 1025s, 770s, 750s, 725s. Anal. Calc. for $C_{19}H_{20}O$: C, 86.32; H, 7.63. Found: C, 86.37; H, 7.50%.

4.2. Synthesis of 3-[*o*-CH_3O–C_6H_4–$C(CH_3)(C_2H_5)$]–C_9H_6 (*2*)

Ligand **2** was synthesized similarly to **1** except that 6,6′-methyl,ethyl-benzofulvene was used. Pale orange crystals were obtained in 75%, m.p.: 58–60 °C. ^{1}H-NMR (δ, ppm, $CDCl_3$): 7.39 (m, 2H), 7.19 (ddd, 1H, $^3J = 8.1$ Hz, $^3J = 7.4$ Hz, $^4J = 1.68$ Hz), 7.03 (td, 1H, $^3J = 7.4$ Hz, $^4J = 1.0$ Hz), 6.94 (m, 2H), 6.76 (dd, 1H, $^3J = 8.1$ Hz, $^4J = 1.2$ Hz), 6.65 (d, 1H, $^3J = 7.7$ Hz), 6.33 (t, 1H, $^3J = 2.2$ Hz), 3.39 (s, 3H), 3.36 (d, 2H, $^3J = 2.2$ Hz), 2.42 (m, 1H, $^3J = 7.4$ Hz), 2.11 (m, 1H, $^3J = 7.4$ Hz), 1.63 (s, 3H), 0.70 (t, 3H, $^3J = 7.4$ Hz). MS (*m*/*z*): 278 (25, M^+), 163 (100, $M^+ - C_9H_7^\bullet$). IR (cm^{-1}, KBr): 3070m, 2980m, 2955m, 1599m, 1580m, 1485s, 1465s, 1445s, 1390m, 1380m, 1370m, 1305m, 1285s, 1245s, 1180m, 1150m, 1090m, 1025s, 980m, 920w, 770s, 760s, 725s. Anal. Calc. for $C_{20}H_{22}O$: C, 86.29; H, 7.96. Found: 86.07; H, 7.88%.

4.3. Synthesis of rac-[(η^5-C_9H_6-1-$C(CH_3)_2$–o-C_6H_4–OCH_3)$_2ZrCl_2$]·THF (rac-**1a**) and meso-[(η^5-C_9H_6-1-$C(CH_3)_2$–o-C_6H_4–OCH_3)$_2ZrCl_2$]·THF (meso-**1b**)

To the solution of $ZrCl_4(THF)_2$ (1.619 g, 4.29 mmol) in 50 ml THF, was added at r.t. the solution of lithium salt prepared from ligand **1** (2.264 g, 8.58 mmol) in 80 ml THF and *n*-BuLi (7.6 ml, 8.58 mmol) in *n*-hexane. The reaction mixture was stirred for 24 h and then the solvent was removed in vacuo to give an orange solid. It was extracted with 100 ml CH_2Cl_2 and filtrated. The solvent of the filtrate was removed again under vacuum to give 3.1 g of *rac*-**1a**/*meso*-**1b** mixture. Fractional recrystallization of this solid from THF and petroleum ether afforded pure *rac*-**1a** and *meso*-**1b** sequentially. *rac*-**1a**: orange prismatic crystal, 9.1% (300 mg), m.p.: 215–216 °C. ^{1}H-NMR (δ, ppm, $CDCl_3$): 7.66 (m, 2H-4), 7.51 (dd, 2H-8, $^3J_{9,8} = 7.8$ Hz, $^4J_{10,8} = 1.6$ Hz), 7.21 (m, 2H-7), 7.10 (ddd, 2H-10, $^3J_{11,10} = 8.1$ Hz, $^3J_{9,10} = 7.8$ Hz, $^4J_{8,10} = 1.6$ Hz), 7.06 (m, 2H-5, 2H-6), 6.93 (td, 2H-9, $^3J_{8,9} = 7.8$ Hz, $^3J_{10,9} = 7.8$ Hz, $^4J_{11,9} = 1.1$ Hz), 6.60 (dd, 2H-11, $^3J_{10,11} = 8.1$ Hz, $^4J_{9,11} = 1.1$ Hz), 6.54 (dd, 2H-3, $^3J_{2,3} = 3.3$ Hz, $^5J_{7,3} = 0.8$ Hz), 6.15 (d, 2H-2, $^3J_{3,2} = 3.3$ Hz), 3.75 (t, 4H-19, $^3J_{20,19} = 6.5$ Hz), 3.15 (s, 6H-14), 2.06 (s, 6H-12), 1.90 (s, 6H-13), 1.85 (p, 4H-20, $^3J_{19,20} = 6.5$ Hz). MS (*m*/*z*): 651 (50.10, $M^+ - THF–Cl^\bullet$), 357 (100, $M^+ - THF–L^\bullet–CH_3Cl–CH_4$). IR (KBr, cm^{-1}): 3070w, 2980s, 2930s, 2880m, 2840m, 1599m, 1580m, 1485s, 1460s, 1440s, 1380m, 1365m, 1290m, 1248s, 1150m, 1090m, 1060m, 1030s, 805m, 755s. Anal. Calc. for $C_{42}H_{46}Cl_2O_3Zr$ (760.96): C, 66.29; H, 6.09. Found: C, 66.25; H, 6.25%.

meso-**1b**: yellow needle crystal, 12% (400 mg), m.p.: 185–187 °C. ^{1}H-NMR (δ, ppm, $CDCl_3$): 7.56 (dd, 2H-8, $^3J_{9,8} = 7.8$ Hz, $^4J_{10,8} = 1.5$ Hz), 7.48 (d, 2H-4, $^3J_{5,4} = 8.4$ Hz), 7.16 (ddd, 2H-10, $^3J_{11,10} = 8.1$ Hz, $^3J_{9,10} = 7.8$ Hz, $^4J_{8,10} = 1.5$ Hz), 7.08 (d, 2H-7, $^3J_{6,7} = 8.4$ Hz), 7.03–6.94 (m, 2H-5, 2H-6, 2H-9), 6.78 (d, 2H-2, $^3J_{3,2} = 3.3$ Hz), 6.63 (dd, 2H-11, $^3J_{10,11} = 8.1$ Hz, $^4J_{9,11} = 1.0$ Hz), 6.00 (d, 2H-3, $^3J_{3,1} = 3.3$ Hz), 3.75 (t, 4H-19, $^3J_{20,19} = 6.4$ Hz), 3.13 (s, 6H-14), 1.99 (s, 6H-12), 1.98 (s, 6H-13), 1.85 (p, 4H-20, $^3J_{10,20} = 6.4$ Hz). MS (*m*/*z*): 636 (16, $M^+ - THF–CH_3Cl$), 586 (100, $M^+ - THF–2CH_3Cl$). IR (KBr, cm^{-1}): 3070w, 2980s, 2930s, 2880m, 2840m, 1599m, 1580m, 1485s, 1460s, 1440s, 1380m, 1365m, 1290m, 1248s, 1150m, 1090m, 1050m, 1030s, 810m, 790s, 755s. Anal. Calc. for $C_{42}H_{46}Cl_2O_3Zr$ (760.96): C, 66.29; H, 6.09. Found: C, 65.58; H, 6.13%.

4.4. Syntheses of rac-[(η^5-C_9H_6-1-$C(CH_3)(C_2H_5)$–o-C_6H_4–OCH_3)$_2ZrCl_2$]·1/2THF (rac-**2a**) and meso-[(η^5-C_9H_6-1-$C(CH_3)(C_2H_5)$–o-C_6H_4–OCH_3)$_2ZrCl_2$] (meso-**2b**)

The synthetic method was similar. Except that $ZrCl_4(THF)_2$ (0.9577 g, 2.54 mmol), ligand **2** (1.4108 g, 5.08 mmol), and *n*-BuLi (2.3 ml, 5.08 mmol) were used. After fractional crystallization from THF and petroleum ether, analytical products *rac*-**2a** and *meso*-**2b** were obtained. *Rac*-**2a**: orange needle crystal, yield 10%, m.p.: 206–210 °C. ^{1}H-NMR (δ, ppm, $CDCl_3$): 7.63 (m, 2H-4), 7.51 (dd, 2H-8, $^3J_{9,8} = 7.8$ Hz, $^4J_{10,8} = 1.6$ Hz), 7.11–7.08 (m, 2H-7, 2H-10), 7.01 (m, 2H-5, 2H-6), 6.94 (td, 2H-9, $^3J_{10,9} = 7.8$ Hz, $^3J_{8,9} = 7.8$ Hz, $^4J_{9,11} = 1.1$ Hz), 6.63 (d, 2H-3, $^3J_{2,3} = 3.3$ Hz), 6.54 (dd, 2H-11, $^3J_{10,11} = 8.1$ Hz, $^4J_{9,11} = 1.1$ Hz), 6.14 (d, 2H-2, $^3J_{3,2} = 3.3$ Hz), 3.75 (t, 2H-19, $^3J_{20,19} = 6.6$ Hz), 3.06 (s, 6H-14), 2.54 (m, 2H-15, $^3J_{13,15} = 7.4$ Hz), 2.20 (m, 2H-15, $^3J_{13,15} = 7.4$ Hz), 1.98 (s, 6H-12), 1.85 (p, 2H-20, $^3J_{19,20} = 6.6$ Hz), 0.55 (t, 6H-13, $^3J_{15,13} = 7.4$ Hz). MS (*m*/*z*): 664 (56, $M^+ - 1/2THF–CH_3Cl$), 585 (100, $M^+ - 1/2THF–2CH_3Cl–Et^\bullet$). IR ($cm^{-1}$, KBr): 3070w, 2980s, 2960s, 2880m, 2835m, 1599m, 1580m, 1485s, 1460s, 1440s, 1380m, 1350w, 1330w, 1280m, 1248s, 1200w, 1160w, 1150m, 1095m, 1060m, 1040m, 1030s, 800s, 755s. Anal. Calc. for $C_{40}H_{42}Cl_2O_2Zr·1/2THF$ (753.01): C, 67.00; H, 6.16. Found: C, 67.04; H, 6.44%.

meso-**2b**: yellow crystal, yield 24%, m.p.: 206–207 °C. ^{1}H-NMR (δ, ppm, $CDCl_3$): 7.52 (d, 2H-4, 2H-8), 7.14 (ddd, 2H-10, $^3J_{11,10} = 8.1$ Hz, $^3J_{9,10} = 7.8$ Hz, $^4J_{8,10} = 1.55$ Hz), 7.00–6.96 (m, 2H-7, 2H-5), 6.93–6.90 (m, 2H-6, 2H-9), 6.88 (d, 2H-2, $^3J_{3,2} = 3.3$ Hz), 6.55 (dd, 2H-11, $^3J_{10,11} = 8.1$ Hz, $^4J_{9,11} = 1.1$ Hz), 6.07 (d, 2H-3, $^3J_{2,3} = 3.3$ Hz), 3.01 (s, 6H-14), 2.86 (m, 2H-15, $^3J_{13,15} = 7.4$ Hz), 2.37 (m, 2H-15, $^3J_{13,15} = 7.4$ Hz), 1.90 (s, 6H-12), 0.71 (t, 6H-13, $^3J_{15,13} = 7.4$ Hz). MS (*m*/*z*): 664 (7, $M^+ - CH_3Cl$), 585 (57, $M^+ - 2CH_3Cl–Et^\bullet$). IR (KBr, cm^{-1}): 3100w, 3070w, 3030w, 2970s, 2935s, 2880m, 2830m, 1599m, 1580m, 1485s, 1460s, 1445s, 1380m, 1350w, 1330w, 1290m, 1248s, 1180w, 1150m, 1095m, 1040m, 1030s, 1000m, 870w, 790s, 755s. Anal. Calc. for $C_{40}H_{42}Cl_2O_2Zr$ (716.91): C, 67.02; H, 5.91. Found: C, 66.93; H, 6.20%.

4.5. X-ray crystallography

The crystal data of *rac*-**1a** were collected on a Rigaku AFC-7R single crystal diffractometer at 293 K using Mo–K_α radiation ($\lambda = 0.71069$ Å, graphite monochromatized, scan type $\omega/2\theta$). Intensities were corrected for Lorentz-polarization effect; an empirical psi-scans correction was applied (0.7521–1.0000). Unit cell parameters were initially obtained from 25 reflections ($14.50 < \theta < 22.43$). The structure was solved primarily by the direct methods using SHELXS-97 system and refined by full-matrix least-squares on F^2 using all of the reflections with SHELXL-97 program. Hydrogen atoms were solved geometrically and refined with mixed methods. Crystal data for *rac*-**1a**: $C_{38}H_{38}Cl_2O_2Zr·C_4H_8O$, $M = 760.95$, prismatic orange crystal; crystal dimensions, $0.20 \times 0.22 \times 0.25$ mm; orthorhombic, $a = 12.910(3)$, $b = 12.622(4)$, $c = 23.040(4)$ Å, $V =$

3754.4(16) Å^3, space group *Pbcn* (# 60), $Z = 4$, $D_{calc} = 1.346$ g cm^{-3}, $F(000) = 1584.00$, $\mu(Mo-K_\alpha) = 0.209$ cm^{-1}, $T = 293$ K; of 3268 reflections measured, all are independent. Number of reflections and parameters in refinement are 3268, and 219. Goodness-of-fit, and the weighted R factor based on F^2 are 1.035 and 0.1834; final R inicate based on F for all data is 0.0859.

5. Supplementary material

Crystallographic data for the structural analysis have been deposited with the Cambridge Crystallographic Data Centre, CCDC No. 164332 for complex *rac*-**1a**. Copies of this information may be obtained free of charge from The Director, CCDC, 12 Union Road, Cambridge CB2 1EZ, UK (Fax: +44-1223-336033; e-mail: deposit@ccdc.cam.ac.uk or www: http://www.ccdc.cam.ac.uk). ^{1}H–^{1}H TOCSY and NOESY spectra of *meso*-**1b** are available.

Acknowledgements

We gratefully acknowledge the financial support from Special Funds for Major State Basic Research Projects (G1999064801) and National Natural Science Foundation of China (20072004).

References

[1] A.L. McKnight, R.M. Waymouth, Chem. Rev. 98 (1998) 2587.
[2] S.D. Ittel, L.K. Johnson, M. Brookhart, Chem. Rev. 100 (2000) 1169.
[3] H.G. Alt, A. Köppl, Chem. Rev. 100 (2000) 1205.
[4] G.W. Coates, Chem. Rev. 100 (2000) 1223.
[5] L. Resconi, L. Cavallo, A. Fait, F. Piemontesi, Chem. Rev. 100 (2000) 1253.
[6] (a) H. Schnutenhaus, H.H. Brintzinger, Angew. Chem. Int. Ed. Engl. 18 (1979) 777;
(b) F.R.W.P. Wild, L. Zsolnai, G. Huttner, H.H. Brintzinger, J. Organomet. Chem. 232 (1982) 233.
[7] (a) H. Sinn, W. Kaminsky, Adv. Organomet. Chem. 18 (1980) 99;
(b) W. Kaminsky, K. Külper, H.H. Brintzinger, F.R.W.P. Wild, Angew. Chem. 97 (1985) 507.
[8] (a) J.A. Even, J. Am. Chem. Soc. 106 (1984) 6355;
(b) J.A. Even, R.L. Lones, A. Razavi, J.D. Ferrara, J. Am. Chem. Soc. 110 (1988) 6255.
[9] (a) L. Resconi, F. Piemontesi, I. Camurati, O. Sudmeijer, I.E. Nifant'ev, P.V. Ivchenko, L.G. Kuz'mina, J. Am. Chem. Soc. 120 (1998) 2308;
(b) M. Toto, L. Cavallo, P. Corradini, G. Moscardi, L. Resconi, G. Guerra, Macromolecules 31 (1998) 3431;
(c) L. Resconi, D. Balboni, G. Baruzzi, C. Fiori, S. Guidotti, P. Mercandelli, A. Sironi, Organometallics 19 (2000) 420.
[10] (a) G.W. Coates, R.M. Waymouth, Science 267 (1995) 217;
(b) E. Hauptman, R.M. Waymouth, J.W. Ziller, J. Am. Chem. Soc. 117 (1995) 11586;
(c) R. Kravchenko, A. Masood, R.M. Waymouth, Organometallics 16 (1997) 5909;
(d) M.D. Bruce, G.W. Coates, E. Hauptman, R.M. Waymouth, J.W. Ziller, J. Am. Chem. Soc. 119 (1997) 11174;
(e) C.D. Tagge, R.L. Kravchenko, T.K. Lal, R.M. Waymouth, Organometallics 119 (1999) 380.
[11] (a) G. Erker, B. Temme, J. Am. Chem. Soc. 114 (1992) 4004;
(b) G. Erker, M. Aulbach, M. Knickmeier, D. Wingbermühle, C. Kruger, M. Nolte, S. Werner, J. Am. Chem. Soc. 115 (1993) 4590.
[12] C. Krüger, F. Lutz, M. Notle, G. Erker, M. Aulbach, J. Organomet. Chem. 452 (1993) 79.
[13] N.E. Grimmer, N.J. Coville, C.B. de Koning, J.M. Smith, L.M. Cook, J. Organomet. Chem. 616 (2000) 112.
[14] G. Jany, M. Gustafsson, T. Repo, E. Aitola, J.A. Dobado, M. Klinga, M. Leskelä, J. Organomet. Chem. 553 (1998) 173.
[15] G.Y. Lee, M. Xue, M.S. Kang, O.C. Kwon, J.-S. Yoon, Y.-S. Lee, H.S. Kim, H. Lee, I.-M. Lee, J. Organomet. Chem. 558 (1998) 11.
[16] M. Knickmeier, G. Erker, T. Fox, J. Am. Chem. Soc. 118 (1996) 9623.
[17] (a) K.J. Stone, R.D. Little, J. Org. Chem. 49 (1984) 1849;
(b) H.G. Alt, M. Jung, G. Kehr, J. Organomet. Chem. 562 (1998) 153.
[18] H. Ma, J. Huang, Y. Qian, Inorg. Chem. Comm. 4 (2001) 515.
[19] H. Ma, J. Huang, Y. Qian, unpublished results.
[20] B.J. Grimmond, J.Y. Corey, N.P. Rath, Organometallics 18 (1999) 404.
[21] (a) A.A.H. van der Zeijden, C. Mattheis, Organometallics 16 (1997) 2651;
(b) A.A.H. van der Zeijden, C. Mattheis, J. Organomet. Chem. 584 (1999) 274;
(c) A.H. van der Zeijden, C. Mattheis, R. Fröhlich, Chem. Ber./Recl. 130 (1997) 1231.
[22] R.L. Halterman, D.R. Fahey, E.F. Bailly, D.W. Docker, O. Stenzel, J.L. Shipman, M.A. Khan, S. Dechert, H. Shumann, Organometallics 19 (2000) 5464.
[23] S. Knüppel, J.-L. Fauré, G. Erker, G. Kehr, M. Nissinen, R. Fröhlich, Organometallics 19 (2000) 1262.
[24] R. Leino, H.J.G. Luttikhedde, A. Lehtonen, R. Sillanpää, A. Penninkangas, J. Strandén, J. Mattinen, J.H. Näsman, J. Organomet. Chem. 558 (1998) 171.
[25] B.S. Furniss, et al., Vogel's Textbook of Practical Organic Chemistry, 4th ed., Longman, 1987.